The Journal of Chemical Physics

Time reversal symmetry breaking and odd viscosity in active fluids: Green–Kubo and NEMD results

Cite as: J. Chem. Phys. **152**, 201102 (2020); https://doi.org/10.1063/5.0006441
Submitted: 05 March 2020 . Accepted: 30 April 2020 . Published Online: 22 May 2020

Cory Hargus, Katherine Klymko, Jeffrey M. Epstein, and Kranthi K. Mandadapu

The Journal of Chemical Physics COMMUNICATION scitation.org/journal/jcp

Time reversal symmetry breaking and odd viscosity in active fluids: Green–Kubo and NEMD results

Cite as: J. Chem. Phys. 152, 201102 (2020); doi: 10.1063/5.0006441
Submitted: 5 March 2020 • Accepted: 30 April 2020 •
Published Online: 22 May 2020

Cory Hargus,[1,a)] Katherine Klymko,[2] Jeffrey M. Epstein,[3] and Kranthi K. Mandadapu[1,4,b)]

AFFILIATIONS

[1]Department of Chemical and Biomolecular Engineering, University of California, Berkeley, California 94720, USA
[2]Computational Research Division, Lawrence Berkeley National Laboratory, Berkeley, California 94720, USA
[3]Department of Physics, University of California, Berkeley, California 94720, USA
[4]Chemical Sciences Division, Lawrence Berkeley National Laboratory, Berkeley, California 94720, USA

[a)]hargus@berkeley.edu
[b)]**Author to whom correspondence should be addressed:** kranthi@berkeley.edu

ABSTRACT

Active fluids, which are driven at the microscale by non-conservative forces, are known to exhibit novel transport phenomena due to the breaking of time reversal symmetry. Recently, Epstein and Mandadapu [arXiv:1907.10041 (2019)] obtained Green–Kubo relations for the full set of viscous coefficients governing isotropic chiral active fluids, including the so-called odd viscosity, invoking Onsager's regression hypothesis for the decay of fluctuations in active non-equilibrium steady states. In this Communication, we test these Green–Kubo relations using molecular dynamics simulations of a canonical model system consisting of actively torqued dumbbells. We find the resulting odd and shear viscosity values from the Green–Kubo relations to be in good agreement with values measured independently through non-equilibrium molecular dynamics flow simulations. This provides a test of the Green–Kubo relations and lends support to the application of the Onsager regression hypothesis in relation to viscous behaviors of active matter systems.

INTRODUCTION

Statistical physics has traditionally been concerned with systems at equilibrium. A natural generalization pursued by Onsager, Prigogine, de Groot and Mazur, and others is to consider systems that are globally out of equilibrium but that obey the local equilibrium hypothesis.[2–6] Such systems model transport phenomena allowing linear laws, such as those of Fourier and Fick, to be derived from the principles of equilibrium thermodynamics and statistical mechanics.[4,5,7] The physical origin of the non-equilibrium nature of these systems is driving at boundaries, as in a rod heated from one end or a channel connecting regions of different solute concentrations.

A more radical departure from equilibrium is achieved in active matter systems in which equilibrium is broken at the local level by non-conservative microscopic forces. Such activity is known to modify existing phase behavior and give rise to qualitatively new dynamical phases, as in motility-induced phase separation.[8,9] Similarly, activity not only modifies existing transport coefficients but can lead to entirely new coefficients, such as the odd (or Hall) viscosity appearing in chiral active fluids.[1,10–15]

Recent work by Epstein and Mandadapu[1] reveals that odd viscosity arises in two-dimensional chiral active fluids due to the breaking of time reversal symmetry at the level of stress correlations. This is demonstrated by a set of Green–Kubo relations derived through the application of the Onsager regression hypothesis.[4,5,7] In this Communication, we evaluate these Green–Kubo relations using molecular dynamics simulations of a model system composed of microscopically torqued dumbbells, finding them to be in good agreement with non-equilibrium molecular dynamics (NEMD) flow simulations across a wide range of densities and activities (Fig. 4).

THEORY

We begin by reviewing the continuum theory for two-dimensional viscous active fluids with internal spin. This provides the setting for the derivation of Green–Kubo relations for viscosity coefficients in fluids breaking time reversal symmetry. Because the chiral active dumbbell model considered in this paper is capable of storing angular momentum in the form of internal (i.e. molecular) spin, we anticipate possible coupling between a velocity field v_i and a spin field m. These satisfy balance equations for linear and angular momentum, as proposed by Dahler and Scriven,[16]

$$\rho \dot{v}_i = T_{ij,j} + \rho g_i, \tag{1}$$

$$\rho \dot{m} = C_{i,i} - \epsilon_{ij} T_{ij} + \rho G. \tag{2}$$

T_{ij} denotes the stress tensor and C_i denotes the spin flux, which accounts for transfer of internal angular momentum across surfaces. The variables g_i and G denote body forces and body torques, respectively. Finally, note that the balance of angular momentum includes a term in which the two-dimensional Levi–Civita tensor ϵ_{ij} is contracted with the stress so that the antisymmetric component of the stress may be nontrivial. We use the notation $a_{,i} = \partial a/\partial x_i$.

The most general isotropic constitutive equations for viscous fluids relating T_{ij} and C_i to v_i, m, and their derivatives up to first order in two-dimensional systems are given by

$$T_{ij} = \eta_{ijkl} v_{k,l} + \gamma_{ij} m - p\delta_{ij} + p^* \epsilon_{ij}, \tag{3}$$

$$C_i = \alpha_{ij} m_{,j}, \tag{4}$$

where η_{ijkl}, γ_{ij}, and α_{ij} are the viscous transport coefficients.[1] Here, p and p^* are hydrostatic contributions and are not constitutively related to v_i and m. The forms of Eqs. (3) and (4) follow from a general representation theorem stating that any isotropic tensor can be expressed in a basis consisting of contractions of Kronecker tensors δ_{ij} and Levi–Civita tensors ϵ_{ij} and that, consequently, there exist no isotropic tensors of odd rank in two dimensions. Thus, the transport coefficients may be expressed as

$$\eta_{ijkl} = \sum_{n=1}^{6} \lambda_n s^{(n)}_{ijkl}, \tag{5}$$

$$\gamma_{ij} = \gamma_1 \delta_{ij} + \gamma_2 \epsilon_{ij}, \tag{6}$$

$$\alpha_{ij} = \alpha_1 \delta_{ij} + \alpha_2 \epsilon_{ij}, \tag{7}$$

where Table I contains the definitions of tensors $s^{(n)}_{ijkl}$.

The coefficients γ_n and α_n indicate the responses of the stress and spin flux tensors to spin and spin gradients. λ_1 and λ_2 are the typical bulk and shear viscosities. λ_3 is the rotational viscosity indicating resistance to vorticity and giving rise to an anti-symmetric stress, while λ_4 is the so-called odd viscosity quantifying response to shear with a tension or compression in the orthogonal direction. λ_5 and λ_6 correspond to an anti-symmetric pressure from compression and isotropic pressure from vorticity, respectively. Note that non-vanishing λ_3 or λ_6 violates objectivity (independence of stress from vorticity), while non-vanishing λ_3 or λ_5 violates symmetry of the stress tensor.

TABLE I. Basis of isotropic rank four tensors in two dimensions appearing in Eq. (5). Adapted from Ref. 1.

Basis tensor	Components
$\mathbf{s}^{(1)}$	$\delta_{ij}\delta_{kl}$
$\mathbf{s}^{(2)}$	$\delta_{ik}\delta_{jl} - \epsilon_{ik}\epsilon_{jl}$
$\mathbf{s}^{(3)}$	$\epsilon_{ij}\epsilon_{kl}$
$\mathbf{s}^{(4)}$	$\epsilon_{ik}\delta_{jl} + \epsilon_{jl}\delta_{ik}$
$\mathbf{s}^{(5)}$	$\epsilon_{ik}\delta_{jl} - \epsilon_{jl}\delta_{ik} + \epsilon_{ij}\delta_{kl} + \epsilon_{kl}\delta_{ij}$
$\mathbf{s}^{(6)}$	$\epsilon_{ik}\delta_{jl} - \epsilon_{jl}\delta_{ik} - \epsilon_{ij}\delta_{kl} - \epsilon_{kl}\delta_{ij}$

Using the conservation and constitutive Eqs. (1), (2), and (5)–(7), Ref. 1 obtains a set of Green–Kubo relations for γ_n and λ_n via invocation of the Onsager regression hypothesis,

$$\gamma_1 = \frac{1}{2\rho_0 \nu} \delta_{ij}\epsilon_{kl}\mathcal{T}^{ijkl}, \tag{8}$$

$$\gamma_2 = \frac{1}{2\rho_0 \nu} \epsilon_{ij}\epsilon_{kl}\mathcal{T}^{ijkl}, \tag{9}$$

$$\lambda_1 + 2\lambda_2 + \lambda_3 - \frac{\gamma_1 \pi}{2\mu} + \frac{\gamma_2 \tau}{2\mu} = \frac{1}{2\rho_0 \mu} \delta_{ik}\delta_{jl}\mathcal{T}^{ijkl}, \tag{10}$$

$$\lambda_4 + \lambda_5 + \lambda_6 - \frac{\gamma_1 \tau}{4\mu} - \frac{\gamma_2 \pi}{4\mu} = \frac{1}{4\rho_0 \mu} \epsilon_{ik}\delta_{jl}\mathcal{T}^{ijkl}, \tag{11}$$

$$\lambda_5 - \frac{\gamma_2 \pi}{4\mu} = \frac{1}{8\rho_0 \mu} \epsilon_{ij}\delta_{kl}\mathcal{T}^{ijkl}, \tag{12}$$

$$\lambda_3 + \frac{\gamma_2 \tau}{2\mu} = \frac{1}{4\rho_0 \mu} \epsilon_{ij}\epsilon_{kl}\mathcal{T}^{ijkl}. \tag{13}$$

$\mathcal{T}^{ijkl}$ is the integrated stress correlation function given by

$$\mathcal{T}^{ijkl} = \int_0^\infty dt \langle \delta T_{ij}(t) \delta T_{kl}(0) \rangle. \tag{14}$$

Note that the stress tensor in (14) is defined as a spatial average, as in the following section. μ, ν, τ, and π are static correlation functions in the non-equilibrium steady state given by

$$\mu \delta_{ij} = \frac{1}{A^2} \int \left\langle \delta v^i(\mathbf{x}) \delta v^j(\mathbf{y}) \right\rangle d^2\mathbf{x}\, d^2\mathbf{y}, \tag{15}$$

$$\pi = \frac{1}{A^2} \int (y^i - x^i) \left\langle \delta v^i(\mathbf{x}) \delta m(\mathbf{y}) \right\rangle d^2\mathbf{x}\, d^2\mathbf{y}, \tag{16}$$

$$\tau = \frac{1}{A^2} \int \epsilon_{kr}(y^r - x^r) \left\langle \delta m(\mathbf{x}) \delta v^k(\mathbf{y}) \right\rangle d^2\mathbf{x}\, d^2\mathbf{y}, \tag{17}$$

$$\nu = \frac{1}{A^2} \int \langle \delta m(\mathbf{x}) \delta m(\mathbf{y}) \rangle d^2\mathbf{x}\, d^2\mathbf{y}, \tag{18}$$

respectively, where A is the area of the system. In particular, μ and ν can be regarded as measuring the effective translation and spin temperatures in the steady state. For equilibrium systems, equipartition implies $\mu = \nu$ and $\pi = \tau = 0$. Finally, the above Green–Kubo relations show that two of the transport coefficients, λ_3 and γ_2, are related by $2\lambda_3 = \gamma_2(\nu - \tau)/\mu$.

For the chiral active dumbbell fluid, the situation is further simplified. As we will show in the following sections, the absence of alignment interactions, i.e. torque interactions acting at a distance between misaligned dumbbells, results in $\gamma_1 = \gamma_2 = 0$, effectively decoupling the velocity from the spin field and also setting $\lambda_3 = 0$. Moreover, symmetry and objectivity of the stress tensor sets two more of the viscosity coefficients to zero, leaving

$$\eta_{ijkl} = \lambda_1(\delta_{ij}\delta_{kl}) + \lambda_2\big(\delta_{ik}\delta_{jl} - \epsilon_{ik}\epsilon_{jl}\big) + \lambda_4\big(\epsilon_{ik}\delta_{jl} + \epsilon_{jl}\delta_{ik}\big). \tag{19}$$

These simplifications also allow us to write simplified Green–Kubo expressions for the shear viscosity,

$$\lambda_2 = \frac{1}{4\rho_0\mu}\int_0^\infty dt\,\langle(\delta T_{22}(t) - \delta T_{11}(t))(\delta T_{22}(0) - \delta T_{11}(0))\rangle, \tag{20}$$

and the odd viscosity,

$$\lambda_4 = \frac{1}{4\rho_0\mu}\int_0^\infty dt[\langle\delta T_{11}(t)\delta T_{21}(0)\rangle - \langle\delta T_{11}(0)\delta T_{21}(t)\rangle + \langle\delta T_{12}(t)\delta T_{22}(0)\rangle - \langle\delta T_{12}(0)\delta T_{22}(t)\rangle], \tag{21}$$

[see Appendix II in the supplementary material for separating the coefficient λ_2 from (10)]. Equation (21) shows that non-vanishing odd viscosity, i.e. $\lambda_4 \neq 0$, requires breaking time reversal symmetry at the level of stress correlation functions, thus breaking the Onsager reciprocal relations.[1,5] Note that (20) is not the typical Green–Kubo expression used to calculate the shear viscosity. However, it can also be rewritten for isotropic systems in the typical form, which are invariant under rotation as

$$\lambda_2 = \frac{1}{\rho_0\mu}\int_0^\infty dt\,\langle\delta T'_{12}(t)\delta T'_{12}(0)\rangle, \tag{22}$$

using a transformation $\boldsymbol{T}' = \boldsymbol{R}^T\boldsymbol{T}\boldsymbol{R}$ corresponding to a rotation $\boldsymbol{R}$ of angle $\pi/4$, for which $T'_{12} = \frac{1}{2}(T_{22} - T_{11})$. The form in (20) is a result of the theory for the choice of the representation theorem for viscous transport coefficients using the basis $s^{(n)}_{ijkl}$.

In the following, we evaluate the shear and odd viscosity Green–Kubo expressions at various densities and driving forces using molecular simulations of chiral active dumbbells in a non-equilibrium steady state. We then subject the dumbbell system to non-uniform shearing flow and evaluate the viscosity coefficients independently. Such an analysis will provide support to both the application of Onsager's regression hypothesis to fluctuations in active non-equilibrium steady states and the ensuing Green–Kubo relations for viscous behaviors of active systems.

MICROSCOPIC MODEL

Chiral active dumbbells

We consider a fluid composed of dumbbells subject to active torques,[17] as shown in Fig. 1. Each dumbbell is composed of two

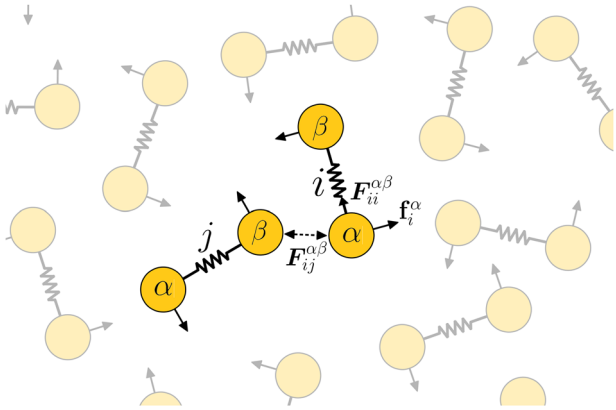

FIG. 1. A two-dimensional fluid composed of chiral active dumbbells. In addition to interacting with its neighbors, each dumbbell is rotated counterclockwise by equal and opposite active forces $\mathbf{f}^{\alpha}_i$.

particles of unit mass connected by a harmonic spring. The system evolves according to underdamped Langevin dynamics

$$\begin{aligned}\dot{\boldsymbol{x}}^{\alpha}_i &= \boldsymbol{v}^{\alpha}_i,\\ \dot{\boldsymbol{v}}^{\alpha}_i &= \sum_{j\beta}\boldsymbol{F}^{\alpha\beta}_{ij} + \mathbf{f}^{\alpha}_i + \boldsymbol{g}^{\alpha}_i - \zeta\boldsymbol{v}^{\alpha}_i + \boldsymbol{\eta}^{\alpha}_i,\end{aligned} \tag{23}$$

with indices $i, j \in [1, N]$ and $\alpha, \beta \in \{1, 2\}$ running over dumbbells and particles, respectively. Variables $\boldsymbol{x}^{\alpha}_i$ and $\boldsymbol{v}^{\alpha}_i$ represent atom positions and velocities. ζ is the dissipative substrate friction and T is the substrate temperature determining the variance of the random thermal force $\boldsymbol{\eta}^{\alpha}_i(t)$, modeled as Gaussian white noise affecting each particle independently such that, indicating vector components with indices a and b, we have $\langle\eta^{\alpha}_{ia}(t)\eta^{\beta}_{jb}(t')\rangle = 2k_BT\zeta\delta(t - t')\delta_{ab}\delta_{ij}\delta_{\alpha\beta}$. Particles in different dumbbells interact through a pairwise Weeks-Chandler-Andersen (WCA) potential,[18] resulting in interaction forces $\boldsymbol{F}^{\alpha\beta}_{ij}$. The particles in a dumbbell are subjected to equal and opposite non-conservative active forces $\mathbf{f}^{\alpha}_i$, which satisfy $\mathbf{f}^1_i = -\mathbf{f}^2_i := \mathbf{f}_i$, and are always perpendicular to the bond vector $\boldsymbol{d}_i = \boldsymbol{x}^1_i - \boldsymbol{x}^2_i$. This imposes an active torque at the level of individual dumbbells. Finally, $\boldsymbol{g}^{\alpha}_i = \boldsymbol{g}(\boldsymbol{x}^{\alpha}_i)$ is an optional externally imposed body force and will be employed later in Poiseuille flow simulations to test the Green–Kubo relations.

Previous work[17] used the Irving–Kirkwood procedure to coarse-grain the microscopic Eq. (23) and derive the equations of hydrodynamics, including balance of mass, linear momentum, and angular momentum, as also employed in the context of measuring odd viscosity by Ref. 13. This coarse-graining procedure yields expressions for the stress tensor in terms of molecular variables and active forces. In particular, it is found that applying active forces at the microscale results in an asymmetric stress tensor at the continuum scale given by

$$\boldsymbol{T} = \boldsymbol{T}^{\mathrm{K}} + \boldsymbol{T}^{\mathrm{V}} + \boldsymbol{T}^{\mathrm{A}}, \tag{24}$$

where

$$\boldsymbol{T}^{\mathrm{K}} = -\frac{1}{A}\sum_{i,\alpha} m^{\alpha}_i\boldsymbol{v}^{\alpha}_i \otimes \boldsymbol{v}^{\alpha}_i, \tag{25}$$

$$\boldsymbol{T}^{\mathrm{V}} = -\frac{1}{2A}\sum_{i,j,\alpha,\beta} \boldsymbol{F}_{ij}^{\alpha\beta} \otimes \boldsymbol{x}_{ij}^{\alpha\beta}, \tag{26}$$

$$\boldsymbol{T}^{\mathrm{A}} = -\frac{1}{A}\sum_{i} \mathbf{f}_i \otimes \boldsymbol{d}_i \tag{27}$$

denote the kinetic, virial, and active contributions, respectively.

The active force vector $\mathbf{f}_i$ is related to the unit bond vector $\hat{\boldsymbol{d}}_i$ by a rotation $\boldsymbol{R}$ of angle $\pi/2$, i.e.,

$$\mathbf{f}_i = \mathrm{f}\boldsymbol{R}\hat{\boldsymbol{d}}_i. \tag{28}$$

For positive (negative) f, the dumbbells rotate counter-clockwise (clockwise). We find that the steady state time average of $\boldsymbol{T}^{\mathrm{A}}$ is

$$\begin{aligned}\langle \boldsymbol{T}^{\mathrm{A}} \rangle &= -\rho_0 \langle \mathbf{f} \otimes \boldsymbol{d} \rangle \\ &= -\rho_0 \mathrm{f} d \langle \boldsymbol{R}\hat{\boldsymbol{d}} \otimes \hat{\boldsymbol{d}} \rangle = \frac{\rho_0 \mathrm{f} d}{2}\begin{bmatrix} 0 & 1 \\ -1 & 0 \end{bmatrix},\end{aligned} \tag{29}$$

where $d = \langle |\boldsymbol{d}| \rangle$ is the average bond length. Because the dumbbells rotate with no preferred alignment, the antisymmetry of $\langle \boldsymbol{T}^{\mathrm{A}} \rangle$ follows from replacing the time average with a uniformly weighted average over angles of rotation θ. For example,

$$\langle \boldsymbol{R}\hat{\boldsymbol{d}} \otimes \hat{\boldsymbol{d}} \rangle_{21} = \langle \hat{d}_1 \hat{d}_1 \rangle = \frac{1}{2\pi}\int_0^{2\pi} d\theta \, \cos^2(\theta) = \frac{1}{2}, \tag{30}$$

while the diagonal elements are zero. This shows that the antisymmetric hydrostatic-like term p^* introduced in (3) arises in a non-equilibrium steady state of the active dumbbell model due to the presence of active rotational forces and has the magnitude $p^* = \rho_0 \mathrm{f} d/2$. We further relate p^* to a non-dimensional Péclet number describing the ratio of active rotational forces to thermal fluctuations due to the substrate bath held at temperature T,

$$\mathrm{Pe} = \frac{2\mathrm{f}d}{k_{\mathrm{B}}T} = \frac{4p^*}{\rho_0 k_{\mathrm{B}} T}. \tag{31}$$

We use Pe as defined in (31) to vary the activity in the system when evaluating the transport coefficients.

Green–Kubo calculations

Steady-state molecular dynamics simulations[19] allow direct measurement of the integrated stress correlation functions $\mathcal{T}_{ijkl}$ defined in (14), which are required for the evaluation of the viscous transport coefficients using the Green–Kubo Eqs. (8)–(13).[20] We find that several of these coefficients vanish in the non-equilibrium steady states at all simulated activities and densities due to cancellations of the correlation functions (see Appendix Fig. A1 in the supplementary material). In particular,

$$\epsilon_{ij}\epsilon_{kl}\mathcal{T}_{ijkl} = \delta_{ij}\epsilon_{kl}\mathcal{T}_{ijkl} = \epsilon_{ij}\delta_{kl}\mathcal{T}_{ijkl} = 0. \tag{32}$$

This immediately implies $\gamma_1 = \gamma_2 = \lambda_3 = \lambda_5 = \lambda_6 = 0$ so that the stress tensor is symmetric and objective. It now remains to evaluate the two non-trivial transport coefficients λ_2 and λ_4 using (20) and (21). For these coefficients, we compute the effective translation temperature as $(A\rho_0)\mu = m\langle (v_i^{\alpha})^2 \rangle$, consistent with the stress tensor defined in (24)–(27).

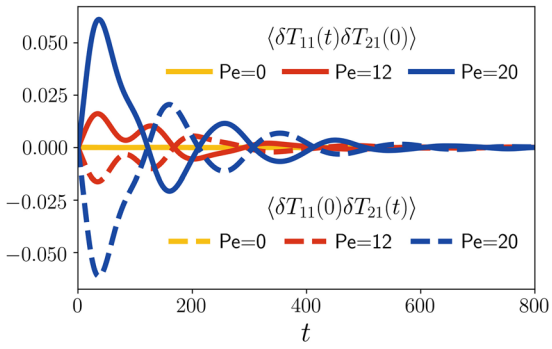

FIG. 2. Stress correlation functions contributing to the odd viscosity ($\rho_0 = 0.4$). For Pe ≠ 0, these correlation functions display time reversal antisymmetry, adding constructively to yield a nonzero odd viscosity.

Figure 2 shows the stress correlation functions $\langle \delta T_{11}(t)\delta T_{21}(0) \rangle$ and $\langle \delta T_{11}(0)\delta T_{21}(t) \rangle$ for various Pe. These are typically zero for systems in equilibrium but become nonzero in the chiral active dumbbell fluid for Pe ≠ 0. In general, we find

$$\begin{aligned}\langle \delta T_{11}(t)\delta T_{21}(0) \rangle &= -\langle \delta T_{11}(0)\delta T_{21}(t) \rangle \\ &= -\langle \delta T_{11}(-t)\delta T_{21}(0) \rangle,\end{aligned} \tag{33}$$

where the final equality is due to stationarity. The analogous equations are satisfied by $\langle \delta T_{12}(t)\delta T_{22}(0) \rangle$. Due to this time reversal antisymmetry, these correlation functions add constructively, yielding a non-vanishing odd viscosity from the Green–Kubo relation (21).

Figure 4 shows the Green–Kubo estimates for λ_2 and λ_4 for various activities and for a range of low to high densities. We find that the shear viscosity increases with density as well as with activity. The dependence of the odd viscosity on activity, while apparently linear at low density, becomes increasingly sigmoidal at high density. Because the sign of Pe controls the direction of active rotation, the time reversal symmetry and antisymmetry, respectively, of λ_2 and λ_4 in Eqs. (20) and (21) require that λ_2 must be

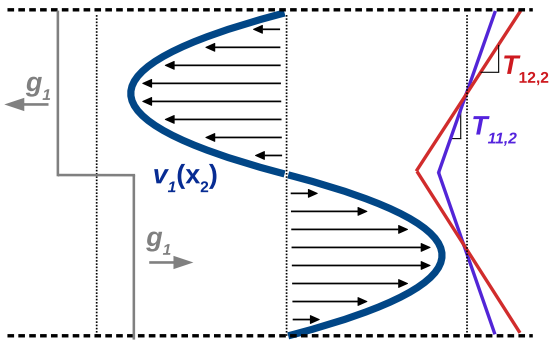

FIG. 3. A schematic of the periodic Poiseuille non-equilibrium molecular dynamics (NEMD) simulation method. The top half of the system is subjected to a uniform body force to the left and the bottom half to a uniform body force of equal magnitude to the right. This yields a parabolic velocity profile and, for odd viscous fluids, an atypical normal stress T_{11}.

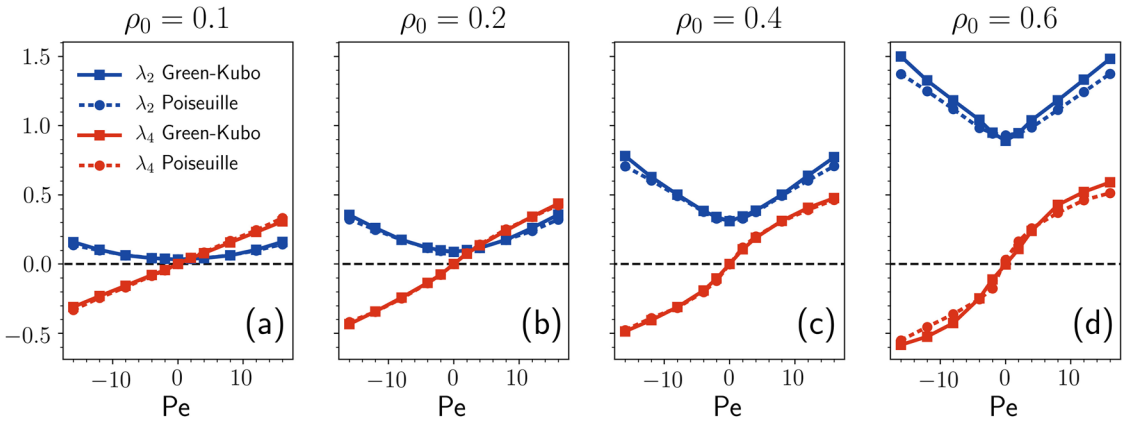

FIG. 4. Comparison of shear viscosity (λ_2) and odd viscosity (λ_4) values obtained from the Green–Kubo relations (solid lines) with those obtained from periodic Poiseuille NEMD simulations (dashed lines). Error bars due to sampling convergence are smaller than the symbols. Figures (a)–(d) show this comparison at densities $\rho_0 \in \{0.1, 0.2, 0.4, 0.6\}$, respectively. Each figure scans over Pe $\in \{-16, -12, -8, -4, -2, 0, 2, 4, 8, 12, 16\}$.

an even function of Pe, while λ_4 must be odd. Note that the odd viscosity, as a non-dissipative transport coefficient, may be negative without introducing an inconsistency with the second law of thermodynamics.

Poiseuille flow NEMD simulations

To verify the values computed from the Green–Kubo formulas, (20) and (21), we measure λ_2 and λ_4 independently via non-equilibrium molecular dynamics simulations. To this end, we simulate plane Poiseuille-like flow via the inclusion of a nonzero body force $\boldsymbol{g}$ in (23) according to the periodic Poiseuille method.[21] As depicted in Fig. 3, we apply equal and opposite uniform body forces of magnitude g_1 in the x_1 direction across a rectangular channel of width $2L$, compatible with periodic boundary conditions. In the following analysis, we consider only the bottom half of the system depicted in Fig. 3, as the top half is symmetrically identical.

The setup in Fig. 3 represents a non-trivial boundary value problem, which not only yields non-uniform flows and non-uniform stresses but also provides a stringent test for the expected constitutive behaviors of the active dumbbell fluid and the estimates of the transport coefficients obtained from Green–Kubo formulas. The velocity profile and pressure profile for flow driven by a small, uniform body force can be solved analytically from the continuum theory, yielding

$$v_1(x_2) = \frac{\rho_0 g_1}{2\lambda_2} x_2 (L - x_2) \tag{34}$$

and

$$p(x_2) = \frac{\lambda_4}{\lambda_2} \rho_0 x_2 g_1 + p_0, \tag{35}$$

respectively, where p_0 is an arbitrary reference pressure (see Appendix IV in the supplementary material for the solution to the corresponding boundary value problem). Our simulations of active dumbbell fluids are consistent with these profiles for various densities and activities (see Appendix Fig. A3 in the supplementary material). Given the velocity and pressure profiles in (34) and (35), the shear and odd viscosities can be computed from the expressions

$$\lambda_2 = \frac{\rho_0 g_1 L^2}{12 \bar{v}}, \tag{36}$$

$$\lambda_4 = \frac{T_{11,2}}{2 v_{1,22}} = -\frac{\lambda_2 T_{11,2}}{2 \rho_0 g_1}, \tag{37}$$

respectively, where $\bar{v} = \frac{1}{L} \int_0^L dx_2 \, v_1(x_2)$ (see Appendix IV in the supplementary material). The slope of the stress component T_{11} can be identified in molecular simulations using the Irving–Kirkwood expression (24)–(27).

The shear and odd viscosities calculated using this NEMD approach are found to be in agreement with the Green–Kubo predictions for a wide range of densities and Péclet numbers (see Fig. 4).

DISCUSSION

In this work, we have validated the non-equilibrium Green–Kubo formulas derived in Ref. 1 using molecular dynamics simulations of the chiral active dumbbell model system to show that odd viscosity is a direct consequence of the breaking of time reversal symmetry at the level of stress fluctuations. In doing so, we provide support for the application of the Onsager regression hypothesis to fluctuations about non-equilibrium steady states, which was used to derive these equations. Complementary work by Han *et al.*[15] measures transport coefficients including the odd viscosity in a different model system consisting of frictional granular particles, upon obtaining Green–Kubo relations identical in form to Ref. 1 using a projection operator formalism and finding similar agreement with NEMD measurements. Together with the present work, these results suggest broad applicability of these Green–Kubo relations in active fluids. Future work entails understanding the microscopic origins of the functional dependence of the viscosities with density and activity.

SUPPLEMENTARY MATERIAL

See the Appendix in the supplementary material for details of the simulation methodology and derivations related to the Green–Kubo relations and Poiseuille-like flow in the presence of odd viscosity.

ACKNOWLEDGMENTS

C.H. was supported by the National Science Foundation Graduate Research Fellowship Program under Grant No. DGE 1752814. K.K.M. was supported by Director, Office of Science, Office of Basic Energy Sciences, of the U.S. Department of Energy under Contract No. DEAC02-05CH11231.

DATA AVAILABILITY

The data that support the findings of this study are available from the corresponding author upon reasonable request.

REFERENCES

[1] J. M. Epstein and K. K. Mandadapu, arXiv:1907.10041 (2019).
[2] S. R. de Groot, *Thermodynamics of Irreversible Processes* (Interscience Publishers Inc., New York, 1951).
[3] S. R. de Groot and P. Mazur, *Non-Equilibrium Thermodynamics* (Dover, New York, 1984).
[4] L. Onsager, Phys. Rev. **37**, 405 (1931).
[5] L. Onsager, Phys. Rev. **38**, 2265 (1931).
[6] I. Prigogine, *Introduction to Thermodynamics of Irreversible Processes* (Wiley-Interscience, New York, 1967).
[7] R. Kubo, M. Yokota, and S. Nakajima, J. Phys. Soc. Jpn., Part 1 **12**, 1203 (1957).
[8] J. Tailleur and M. E. Cates, Phys. Rev. Lett. **100**, 218103 (2008).
[9] M. E. Cates and J. Tailleur, Annu. Rev. Condens. Matter Phys. **6**, 219 (2015).
[10] D. Banerjee, A. Souslov, A. G. Abanov, and V. Vitelli, Nat. Commun. **8**, 1573 (2017).
[11] S. Ganeshan and A. G. Abanov, Phys. Rev. Fluids **2**, 094101 (2017).
[12] A. Souslov, K. Dasbiswas, M. Fruchart, S. Vaikuntanathan, and V. Vitelli, Phys. Rev. Lett. **122**, 128001 (2019).
[13] Z. Liao, M. Han, M. Fruchart, V. Vitelli, and S. Vaikuntanathan, J. Chem. Phys. **151**, 194108 (2019).
[14] B. Bradlyn, M. Goldstein, and N. Read, Phys. Rev. B **86**, 245309 (2012).
[15] M. Han, M. Fruchart, C. Scheibner, S. Vaikuntanathan, W. Irvine, J. de Pablo, and V. Vitelli, arXiv:2002.07679 (2020).
[16] J. Dahler and L. Scriven, Nature **192**, 36 (1961).
[17] K. Klymko, D. Mandal, and K. K. Mandadapu, J. Chem. Phys. **147**, 194109 (2017).
[18] J. D. Weeks, D. Chandler, and H. C. Andersen, J. Chem. Phys. **54**, 5237 (1971).
[19] S. J. Plimpton, J. Comput. Phys. **117**, 1 (1995), see also http://lammps.sandia.gov/.
[20] See https://github.com/mandadapu-group/active-matter for simulation and analysis code used in this Communication.
[21] J. A. Backer, C. P. Lowe, H. C. Hoefsloot, and P. D. Iedema, J. Chem. Phys. **122**, 154503 (2005).